J. Fluid Mech. (2009), *vol.* 625, *pp.* 387–410.
doi:10.1017/S0022112009005771 Printed in the United Kingdom

Rayleigh–Taylor and Richtmyer–Meshkov instabilities of flat and curved interfaces

R. KRECHETNIKOV†

University of California, Santa Barbara, CA 93106, USA

(Received 16 April 2008 and in revised form 18 December 2008)

In this work we discuss a non-trivial effect of the interfacial curvature on the stability of uniformly and suddenly accelerated interfaces, such as liquid rims. The new stability analysis is based on operator and boundary perturbation theories and allows us to treat the Rayleigh–Taylor and Richtmyer–Meshkov instabilities as a single phenomenon and thus to understand the interrelation between these two fundamental instabilities. This leads, in particular, to clarification of the validity of the original Richtmyer growth rate equation and its crucial dependence on the frame of reference. The main finding of this study is the revealed and quantified influence of the interfacial curvature on the growth rates and the wavenumber selection of both types of instabilities. Finally, the systematic approach taken here also provides a generalization of the widely accepted *ad hoc* idea, due to Layzer (*Astrophys. J.*, vol. 122, 1955, pp. 1–12), of approximating the potential velocity field near the interface.

1. Introduction

1.1. *What are the interfacial acceleration-induced instabilities?*

Interfaces either uniformly (Rayleigh 1883; Taylor 1950) or impulsively (Richtmyer 1960; Meshkov 1969) accelerated are ubiquitous in nature and usually exhibit long-wave instabilities and are respectively named after Rayleigh–Taylor (RT) and Richtmyer–Meshkov (RM). In the first case the instability occurs if the light fluid is accelerating the heavy one, while in the second case the instability takes place when an interface between fluids of different density is impulsively accelerated, e.g. by the passage of a shock wave. It is believed, after the work of Richtmyer (1960), that the occurrence of instability in the latter case does not depend upon the direction of impulsive acceleration. These two instabilities are usually studied separately, i.e. without interaction with each other; the known facts on RT and RM instability phenomena were reviewed by Sharp (1984) and Brouillette (2002), accordingly. The physical situations in which the RM instability appears span from combustion (cf. Khokhlov, Oran & Thomas 1999) to astrophysics (cf. Arnett 2000). The RT instability also occurs in various phenomena, e.g. inertial confinement fusion (Lindl & Mead 1975), astrophysics (Frieman 1954; Arons & Lea 1976; Cattaneo & Hughes 1988) and geophysics (Sazonov 1991; Wilcock & Whitehead 1991). Because of this wide fundamental impact, these classical RT and RM instabilities still attract attention: in particular, there are a number of works on the nonlinear analysis of these instabilities, starting with the seminal work of Layzer (1955), who proposed an

† Email address for correspondence: rkrechet@engineering.ucsb.edu

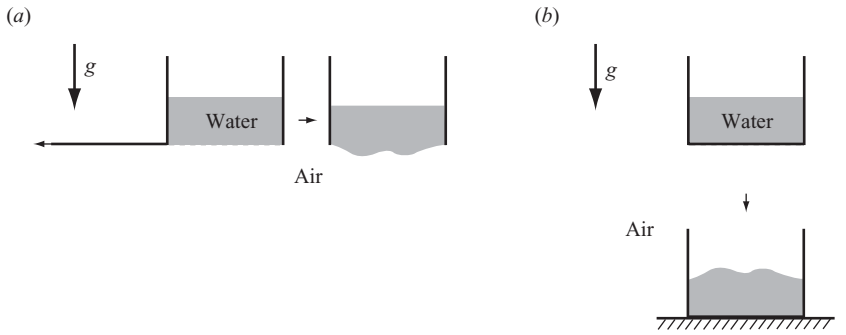

FIGURE 1. Prosaic examples of Rayleigh–Taylor and Richtmyer–Meshkov instabilities. (*a*) A bucket of water with instantaneously removed bottom. (*b*) A bucket of water dropped on the floor.

ad hoc approximation of the velocity potential near the tip of a finger leading to a simple nonlinear model for the finger evolution. This approach has been extended by Ott (1972), Hecht, Alon & Shvarts (1994), Hazak (1996), Velikovich & Dimonte (1996) and Mikaelian (1998). Effects of compressibility were studied by Fraley (1986), Yang, Zhang & Sharp (1994), Mikaelian (1994) and Wouchuk & Nishihara (1996), to name a few. The latter effect can be important in the RM instability, since it often occurs in nature due to a shock propagating through an interface. Also, the effects of viscosity (Carlés & Popinet 2002) and magnetic field (Wouchuk & Nishihara 1996) on the development of the RM instability have been investigated. Despite numerous studies and refinements of both the RT and the RM instabilities, the two key aspects – influence of the frame of reference on the expression for the growth rate and the interfacial curvature on the development of these instabilities – have never been pointed out in the literature. These are the subjects of this work, the motivation for which comes from the recent understanding of the fact that the fundamental instability, which is responsible for the crown formation in the drop splash problem (cf. figure 2), is due to the RM mechanism (Krechetnikov & Homsy 2009), as will be discussed in the next subsection.

Transparent physical examples of both RT and RM instabilities can be given with the help of a bucket of water, as in figure 1. The RT instability would correspond to the case in which the bucket bottom is removed instantaneously, and thus, due to gravity, the water layer is accelerating the air as in figure 1(*a*); another nice visual interpretation of the RT instability was given by Sharp (1984), who considered a water layer plastered to a ceiling. The RM instability would be observed when the same bucket is dropped on the floor so that due to impact the water undergoes a sudden impulsive deceleration, as in figure 1(*b*), and therefore should be stable according to the RT criterion. However, as we know from experience, the water layer becomes unstable. The explanation for this discrepancy between the predictions of the RT and RM criteria comes from the fact that the RM case is the impulsive limit of the RT case. Namely if the interface between two phases is RT unstable under the action of a constant acceleration in one of the directions, then it should be RM unstable in both directions in the non-inertial frame of reference moving with the interface, since in this reference frame it is equally valid to say that the interface is being accelerated from the lighter to the heavier phase and vice versa. Mathematically, this is justified by the fact that the impulsive acceleration, $V_0\delta_D(t)$ with $\delta_D(t)$ being the Dirac delta function, is invariant with respect to the transformation $t \to -t$. Evidently, the view of this

phenomenon in a laboratory frame of reference is not as simple, which will be also demonstrated mathematically in § 2. The clarification of these fundamental frame-dependent properties of the instabilities is naturally important for further studies, in particular, of the effect of interfacial curvature treated in § 3.

The behaviour in the RT case can be described by the time-evolution equation for interfacial perturbations $f(t)$, i.e. deviations from the flat interface, of wavenumber k under constant acceleration g in the coordinate system fixed in the interface

$$\frac{\mathrm{d}^2 f(t)}{\mathrm{d}t^2} = |k|\, g\, f(t), \tag{1.1}$$

which is given for the case in which density of one of the fluids can be neglected, i.e. for unit Atwood number, $A_T = (\rho_1 - \rho_2)/(\rho_1 + \rho_2) = 1$. Apparently, if $g > 0$, then the initially non-zero perturbations will grow exponentially in time. Richtmyer (1960) applied the above Taylor's analysis to the case of impulsive acceleration $g(t) = V_0 \delta_D(t)$, which implies that the interface attains a jump in velocity equal to V_0 at the time instant $t = 0$, i.e. $V(t) = V_0 H(t)$, where $H(t)$ is the Heaviside step function. Integrating (1.1) for such an impulsive acceleration yields the famous Richtmyer growth rate relation

$$\frac{\mathrm{d}f(t)}{\mathrm{d}t} = |k|\, V_0\, f(0), \tag{1.2}$$

which predicts linear growth in time, proportional to the initial amplitude of perturbation f_0 and the velocity jump V_0. It should be stressed that the Richtmyer argument was based on the ingenious generalization of Taylor's result, as developed in the case in which the perturbation 'sits' on the interface, i.e. in the reference frame moving with the interface. While Richtmyer's growth rate relation agrees with the numerical modelling of the compressible case (Yang *et al.* 1994), which was done in the moving frame of reference and with no initial velocity perturbations consistent with Richtmyer's work, and remains the main theoretical model, it consistently predicts a growth rate that is too large compared to experiments (Grove *et al.* 1993). This discrepancy may be due to either nonlinear effects at long times and/or incomplete understanding of the linear case for short times. The focus of this paper is on clarifying the linear theory; namely it will be shown that previous studies were based on a restricted set of initial perturbations and overlooked difference in growths as observed in different reference frames. Thus, as we will see in § 2, the analysis of an impulsively accelerated interface is more complicated than was envisioned by Richtmyer (1960), since the non-trivial nature of the free-surface problems leads to different views of the perturbation evolution in the laboratory frame and the frame moving with the interface, which however can be reconciled (§ 2.6). Also, the systematic approach developed here allows us to demonstrate that the non-zero initial displacement $f(0)$ required for instability is not really necessary, as implied by (1.2) and commonly believed. Because of the time-dependent nature of the basic state – an accelerated flat interface – as well as an impulsive acceleration at $t = 0$, our analysis is based on the Laplace transform methods, since the problem naturally requires treatment as an initial-value problem.

1.2. *Limitations of previous studies and the main result*

While historically the RM instability was studied without an extra effect of constant acceleration (i.e. separately from the RT case), it is intuitively clear that there are no pure impulsive accelerations in the real world and that they are usually combined with constant or slowly changing accelerations. Therefore, it is natural to view both

FIGURE 2. Example of accelerated curved liquid interface: drop splash on thin film.

instabilities as a single phenomenon. This unified understanding will be given in § 2, which uncovers the interaction of these two fundamental instabilities.

Another limitation of the studies of the RT and RM instabilities is connected with the flat-interface base state, in view of its relative ease for analytical treatments. However, there are many physical situations in which curved interfaces are subject to acceleration, e.g. in the drop splash problem (Krechetnikov & Homsy 2009) as illustrated in figure 2. Similar to the depicted case, thin liquid sheets with highly curved edges, which also experience accelerations, are very frequent in various applications, but their stability analysis is not yet available (Sirignano & Mehring 2000). As for the physical origin of impulsive accelerations of such liquid sheets, one mechanism is suggested by figure 2, in which a rim is formed due to a sudden impact. Another possibility for impulsive accelerations is due to body forces, which can be switched on suddenly, such as magnetic and electric fields: they would accelerate not only the interface, as a shock wave would, but also the whole bulk of the liquid.

Given the above physical justifications, our study of these phenomena in the two-dimensional configuration, § 3, reveals a non-trivial effect of non-zero interfacial curvature on the stability characteristics, which can be understood in basic physical terms. Namely, let us re-derive (1.1) for the evolution of an interfacial disturbance of wavenumber k for flat interface, using energy argument. Consider a perturbation of wavenumber k and the liquid column of thickness $\mathrm{d}x$ as dark shaded in figure 3. When the interface is deflected from the flat one, $y=0$, this liquid column respectively attains the changes

$$\Delta \Pi_g = \frac{1}{2} g\rho f^2 \,\mathrm{d}x \quad \text{and} \quad \Delta T \simeq \frac{1}{2}\rho |k|^{-1} \left(\frac{\mathrm{d}f}{\mathrm{d}t}\right)^2 \mathrm{d}x \tag{1.3}$$

in potential and kinetic energies, where in the kinetic energy expression we took into account that the perturbation penetrates into the bulk at the distance $|k|^{-1}$, which is dictated by the solution of Laplace's equation for the velocity potential $\phi \sim \mathrm{e}^{|k|y+\mathrm{i}kx}$

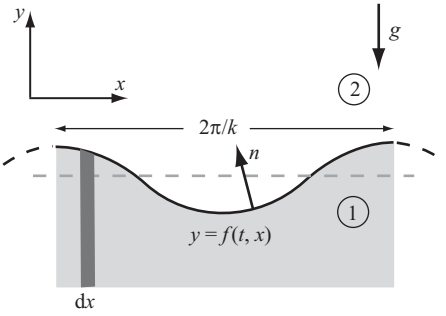

FIGURE 3. Interface between two fluids.

in a half-space, $(x, y) \in \mathbb{R} \times \mathbb{R}^+$ (cf. (2.11)). Thus, the energy form of (1.1) is

$$\left(\frac{\mathrm{d}f}{\mathrm{d}t}\right)^2 + |k|gf^2 = \text{const}, \tag{1.4}$$

and therefore the factor $|k|$ in (1.1) and (1.2) originates from the kinetic energy term. In the case of a curved interface the penetration of a disturbance into the bulk changes, and thus the factor $|k|$ should be replaced with a function of both the wavenumber k and the base-state curvature, which affects not only the perturbation growth rate but also the wavenumber selection. However, formal analysis in this case is more complicated than in the flat-interface base-state case and requires accurate techniques to solve for the velocity potential in a region with curved free boundaries. Resolving this technical difficulty naturally leads to a rigorous generalization of the linear part of the *ad hoc* argument of Layzer (1955), which will be discussed in detail in § 3. Also, intuition regarding the effect of an interfacial curvature developed here will be substantiated by the known example of collapsing underwater bubbles (Birkhoff 1954; Plesset 1954). Finally, the two-dimensional studies will be generalized to three dimensions in § 4. The main results of physical significance are summarized in Assertions 1–4 throughout the text and in brief can be stated as follows.

The interpretation and the growth rate of the Richtmyer–Meshkov instability depend on the frame of reference. The interfacial curvature and its sign influence the growth rates of both the Rayleigh–Taylor and Richtmyer–Meshkov instabilities, as well as the most unstable wavenumber range selection in the transverse direction in the three-dimensional case.

2. Two-dimensional flat interfaces

2.1. *General formulation*

In the analysis of the RT and RM instabilities we adopt the Kelvin's restrictive assumption (Drazin & Reid 2004); i.e. we consider an inviscid and incompressible approximation of irrotational fluids. One can demonstrate that rotational disturbances are no more unstable in the RT case, similar to the argument in chapter 4 of Drazin & Reid (2004); in the RM case, the flow is potential right after the sudden acceleration, since the viscous and inertia forces are not capable of balancing the sudden changes similar to the disk impact problem (Batchelor 1967). Also, as a consequence of the inviscid approximation, the surface tension σ must be taken as constant, since there are no viscous stresses to balance surface tension gradients, i.e. Marangoni stresses (Landau & Lifshitz 1987).

First, consider the two-dimensional configuration of an interface between two fluids in a gravity field $\boldsymbol{g}$, as in figure 3. For simplicity of notation, we consider phase 2 inertialess, while the bulk dynamics in phase 1 are governed by the Euler equations of incompressible fluid of density ρ. In the laboratory Cartesian coordinate frame of reference $(\boldsymbol{i}, \boldsymbol{j})$ these equations are

$$\nabla \cdot \boldsymbol{u} = 0, \tag{2.1a}$$

$$\boldsymbol{u}_t + (\boldsymbol{u}\nabla)\boldsymbol{u} = -\frac{1}{\rho}\nabla p + \boldsymbol{f}, \tag{2.1b}$$

where $\boldsymbol{u} = \boldsymbol{i}\, u + \boldsymbol{j}\, v$ is the velocity field; p is the pressure; and $\boldsymbol{f}$ is the mass force equal to the gravitational acceleration, i.e. $\boldsymbol{f} = -\boldsymbol{j}\, g$. Since the stress tensor $T_{ij} = -p\delta_{ij}$ is inviscid, the only dynamic condition at the interface left is its normal component

$$[\boldsymbol{n} \cdot \boldsymbol{T} \cdot \boldsymbol{n}]_1^2 = \sigma \nabla \boldsymbol{n},$$

where $\boldsymbol{n}$ is the normal unit vector pointing into phase 2. Finally, the system is completed with the kinematic condition, which can be written most conveniently using an implicit representation of the interface, $F = y - f(t, x)$:

$$\frac{\partial F}{\partial t} + \nabla F \cdot \boldsymbol{u} = 0 \implies \frac{\partial f}{\partial t} + u\frac{\partial f}{\partial x} = v \quad \text{on } y = f(t, x). \tag{2.2}$$

Let us also write the dynamic condition in coordinates. If the normal and tangential vectors in the Cartesian coordinates $(\boldsymbol{i}, \boldsymbol{j})$ are

$$\boldsymbol{n} = \frac{\nabla F}{|\nabla F|} = \frac{-\boldsymbol{i} f_x + \boldsymbol{j}}{\sqrt{1 + f_x^2}} \quad \text{and} \quad \boldsymbol{t} = \frac{\boldsymbol{i} + \boldsymbol{j} f_x}{\sqrt{1 + f_x^2}}, \tag{2.3}$$

respectively, then both $(\boldsymbol{i}, \boldsymbol{j})$ and $(\boldsymbol{t}, \boldsymbol{n})$ are right-handed coordinate systems. The normal component of the dynamic condition at the interface becomes

$$p = -\frac{\sigma f_{xx}}{\left(1 + f_x^2\right)^{3/2}} \quad \text{at } y = f(t, x). \tag{2.4}$$

Adopting Kelvin's restrictive assumption that the disturbances flow is irrotational, we introduce the potential ϕ such that $\boldsymbol{u} = \nabla\phi$, which results in the following system for the bulk (the harmonic equation for the potential ϕ and the Lagrange–Cauchy integral for the pressure p) and interfacial dynamics (the normal stress and kinematic conditions):

$$\text{bulk (velocity) } y \leqslant f(t, x): \quad \begin{cases} \Delta\phi = 0, \\ \nabla\phi \to 0, \ \ y \to -\infty, \end{cases} \tag{2.5a}$$

$$\text{bulk (pressure) } y \leqslant f(t, x): \quad \frac{\partial \phi}{\partial t} + \frac{1}{2}\left(\phi_x^2 + \phi_y^2\right) = -\frac{1}{\rho}p - g \cdot y + C(t), \tag{2.5b}$$

$$\text{interface (dynamic) } y = f(t, x): \quad p = -\frac{\sigma f_{xx}}{\left(1 + f_x^2\right)^{3/2}}, \tag{2.5c}$$

$$\text{interface (kinematic) } y = f(t, x): \quad \frac{\partial f}{\partial t} + \frac{\partial \phi}{\partial x}\frac{\partial f}{\partial x} = \frac{\partial \phi}{\partial y}, \tag{2.5d}$$

where $\Delta = \partial_x^2 + \partial_y^2$ is the Laplacian and $C(t)$ is the time-dependent constant in the Lagrange–Cauchy integral (2.5b) to be determined in § 2.2.

2.2. *Base state*

System (2.5) allows us to determine the base state corresponding to the interface, which starts moving with velocity $\boldsymbol{j}\cdot V(t)$ (i.e. in the positive direction of the y-axis) at the initial time instant $t=0$:

$$f^0(t)=\int_0^t V(\widetilde{t})\,\mathrm{d}\widetilde{t}; \tag{2.6}$$

that is there is no x-dependence in view of the flatness of the base-state interface. The kinematic condition (2.5d) then yields the potential function $\phi^0=V(t)y+\alpha(t)$ with some arbitrary time-dependent constant $\alpha(t)$. Since the pressure at the unperturbed, i.e. flat, interface $f^0(t)$ vanishes, cf. (2.5c), the constant $C(t)$ is given by

$$C(t)=\frac{\mathrm{d}\alpha}{\mathrm{d}t}+\left(g+\frac{\mathrm{d}V}{\mathrm{d}t}\right)f^0+\frac{V^2}{2}. \tag{2.7}$$

The Lagrange–Cauchy integral then produces the formula for the base-state pressure

$$p^0=-\rho\left(g+\frac{\mathrm{d}V}{\mathrm{d}t}\right)(y-f^0). \tag{2.8}$$

2.3. *Linearized equations for disturbances*

Introducing linearization around the base state $p=p^0(t,y)+p'(t,x,y)$, $\phi=\phi^0(t,y)+\phi'(t,x,y)$ and the undisturbed interfacial position $f=f^0(t)+f'(t,x)$, we get the following equations for the evolution of disturbances:

$$\frac{\partial\phi'}{\partial t}+V\phi'_y=-\frac{1}{\rho}p',\quad y\leqslant f^0, \tag{2.9a}$$

$$-\rho\left(g+\frac{\mathrm{d}V}{\mathrm{d}t}\right)f'+p'|_{y=f^0}=-\sigma f'_{xx},\quad y=f^0, \tag{2.9b}$$

$$\frac{\partial f'}{\partial t}=\frac{\partial\phi'}{\partial y},\quad y=f^0, \tag{2.9c}$$

while the velocity potential is determined from the free-boundary problem for the Laplace equation:

$$\Delta\phi'=0,\quad y\leqslant f^0, \tag{2.10a}$$

$$\nabla\phi'\to 0,\quad y\to-\infty. \tag{2.10b}$$

Note that in (2.5c) we linearized the pressure in an obvious manner:

$$\begin{aligned}p(t,x,f^0(t)+f'(t,x))&=p^0(t,f^0(t)+f'(t,x))+p'(t,x,f^0(t)+f'(t,x))\\&=p^0(t,f^0(t))+\frac{\partial p^0}{\partial y}(t,f^0(t))\,f'(t,x)+p'(t,x,f^0(t))+\ldots,\end{aligned}$$

which leads to (2.9b).

2.4. *Stability analysis*

Let us denote the Fourier transform of $\phi'(t,x,y)$ in x-variable by $\mathscr{F}(\phi)=\widehat{\phi}(t;k;y)=\int_{-\infty}^{+\infty}\phi'(t,x,y)\,\mathrm{e}^{-ikx}\,\mathrm{d}x$, dropping the prime superscript and, similarly, the Laplace transform in time of $\phi'(t,x,y)$ by $\mathscr{L}(\phi)=\widetilde{\phi}(s;x,y)=\int_{0^-}^{+\infty}\phi'(t,x,y)\,\mathrm{e}^{-st}\,\mathrm{d}t$. Then the combined Fourier–Laplace transform of $\phi'(t,x,y)$ will be denoted by $\overline{\phi}(s;k;y)$. The same notation applies to $f'(t,x)$ and $p'(t,x,y)$.

The solution of (2.10) satisfying the boundary condition at $y \to -\infty$ in the Fourier–Laplace space is

$$\overline{\phi}(s;k;y) = A(s;k)\mathrm{e}^{|k|(y-s\widetilde{f}^0)}, \quad y \leqslant s\,\widetilde{f}^0. \tag{2.11}$$

It is important to stress that since we are studying the stability of the free-boundary problem we need a *general* solution of the Laplace equation (2.10) but not a particular solution with some fixed boundary values. This will have non-trivial implications in § 3, when we will need to construct an analogous solution but in a domain with a curved boundary. Lastly, it is important to note that the solution decays away from the interface exponentially, $\sim \mathrm{e}^{|k|y}$, which will also result in some non-trivial consequences in § 2.5.

Applying the Fourier–Laplace transform to system (2.9), we obtain

$$s\overline{\phi} - \widehat{\phi}(0;k;y) + \mathscr{L}\left[V(t)\frac{\partial\widehat{\phi}}{\partial y}(t;k;y)\right] = -\frac{1}{\rho}\overline{p}, \quad y \leqslant s\cdot\widetilde{f}^0, \tag{2.12a}$$

$$-\rho g\overline{f} - \rho\mathscr{L}\left[\frac{\mathrm{d}V(t)}{\mathrm{d}t}\widehat{f}(t;k)\right] + \overline{p} = \sigma k^2\overline{f}, \quad y = s\cdot\widetilde{f}^0, \tag{2.12b}$$

$$s\overline{f} - \widehat{f}(0;k) = \frac{\mathrm{d}\overline{\phi}}{\mathrm{d}y}, \quad y = s\cdot\widetilde{f}^0, \tag{2.12c}$$

where $\widetilde{f}^0$ is the Laplace transform of $f^0(t)$.

In this work we are interested only in two limiting situations, namely the impulsive acceleration $V(t) = V_0H(t)$ and the constant acceleration, described by $g = \text{const}$. Then the Laplace transforms in (2.12*a*) and (2.12*b*) become $\mathscr{L}[V(t)\frac{\partial\widehat{\phi}}{\partial y}(t;k;y)] = V_0\frac{\mathrm{d}\overline{\phi}}{\mathrm{d}y}$ and $-\rho\mathscr{L}[\frac{\mathrm{d}V(t)}{\mathrm{d}t}\widehat{f}(t;k)] = -\rho V_0\widehat{f}(0;k)$, respectively. Next, after substituting the general solution for the potential (2.11) into (2.12), evaluating (2.12*a*) at the interface and resolving (2.12) for the amplitude $A(s;k)$ by eliminating pressure $\overline{p}$ and the interface $\overline{f}$ disturbances, we find

$$A(s;k) = \frac{s[\widehat{\phi}(0;k;f^0) - V_0\widehat{f}(0;k)] - \left[\sigma\frac{k^2}{\rho} + g\right]\widehat{f}(0;k)}{s^2 + |k|\left[\sigma\frac{k^2}{\rho} + g + sV_0\right]}. \tag{2.13}$$

In order to analyse the asymptotic stability of the original physical system it is not necessary to invert the Fourier and Laplace transforms, but rather one can appeal to the pole diagram analysis, which allows one to determine the long-time behaviour of $\phi(t,x,y)$ based on the knowledge of the location of all the singularities of $\widehat{\phi}(s;k;y)$ in the s-complex plane (Lawrentjew & Schabat 1967). Namely, the rightmost simple poles (i.e. those with largest real part) have the dominant influence on the long-term behaviour of $\phi(t,x,y)$ by dictating the exponential rate of evolution (be it growth or decay); if the rightmost poles are multiple, then algebraic growth is possible; if the real part of the rightmost pole is zero, then nonlinear stability analysis is required. The practical efficiency of this method is that the real part of the coordinate of the rightmost pole is the growth rate λ in the terminology of the standard normal mode (i.e., eigenvalue) analysis; moreover, this approach allows one to capture the algebraic growth as well, while the normal mode analysis fails. Since $\widehat{\phi}(0;k;0)$ and $\widehat{f}(0;k)$ are the initial perturbations in the Fourier space and, in general, arbitrary, then finding poles amounts to the consideration of the vanishing denominator in (2.13) in two situations, when the acceleration is either constant or impulsive:

(*a*) $V_0 = 0$: $s^2 + |k|[\sigma \frac{k^2}{\rho} + g] = 0$ implies that the poles are $s_{1,2} = \pm \sqrt{-|k|(\sigma \frac{k^2}{\rho} + g)}$; i.e. instability takes place for $\sigma \frac{k^2}{\rho} + g < 0$; in other words, g must be less than zero so that there is a range of wavenumbers k, controlled by surface tension, for which the disturbances grow. This is exactly the classical result of Taylor (1950). The rightmost of the above $s_{1,2}$ corresponds to the real part of the leading eigenvalue λ, which controls the time growth $e^{\lambda t}$ and which is shown as the solid curves in figure 9. Equivalently, one can consider the case $dV/dt = a = \text{const}$, which gives the same results as above but with $g \to g + a$.

(*b*) $V_0 \neq 0$: $s^2 + |k|[\sigma \frac{k^2}{\rho} + g + sV_0] = 0$ implies that the poles are located at

$$s_{1,2} = \frac{-|k|V_0 \pm \sqrt{k^2 V_0^2 - 4|k|\left(\sigma \frac{k^2}{\rho} + g\right)}}{2}, \tag{2.14}$$

from which it follows that

(i) if $g < 0$, then linear instability with exponential growth takes place for any V_0;

(ii) if $V_0 < 0$, then one has linear instability with exponential growth;

(iii) if $V_0 > 0$ then one has linear stability for non-zero σ or positive g, and nonlinear stability analysis is required if both σ and g vanish.

From the above the *asymmetry* of the cases $V_0 < 0$ and $V_0 > 0$ is apparent; also the additional effect of constant (not sudden) acceleration is highlighted, which, as one can observe, leads to a non-trivial interaction of the RT and RM instabilities. Also, the presence of surface tension provides stabilization of short wavelengths, as expected. Finally, the growth or decay of the interfacial perturbations is dictated by the stability characteristics of $A(s, k)$ as can be seen from

$$\overline{f}(s;k) = \frac{1}{s}[\widehat{f}(0;k) + A(s;k)|k|] \tag{2.15}$$

because the singularities, which control the growth or decay, are the same as those of $A(s;k)$ discussed above.

Now let us consider the limiting case in which both constant acceleration, g, and surface tension, σ, vanish, i.e. the situation considered originally by Richtmyer (1960). Then the amplitude of the potential and the interfacial perturbations obey

$$A(s;k) = \frac{-V_0 \widehat{f}(0;k) + \widehat{\phi}(0;k;f^0)}{s + |k|V_0}, \quad \overline{f}(s;k) = \frac{s\widehat{f}(0;k) - |k|\widehat{\phi}(0;k;f^0)}{s(s + |k|V_0)}, \tag{2.16}$$

respectively. It is remarkable that the results of the above systematic analysis differ from the standard *ad hoc* conclusions of Richtmyer (1960), who predicted that perturbations should grow algebraically (linearly) in time regardless of the sign of V_0, while our analysis predicts exponential growth for $V_0 < 0$, as follows from (2.16). In order to resolve this discrepancy, let us analyse the perturbation growth in the frame of reference moving with the interface, since historically Richtmyer adopted Taylor's analysis on a moving interface to the case of impulsive acceleration.

2.5. *Analysis in the frame of reference moving with interface*

Let us transform our system to the one moving with the interface with velocity $\boldsymbol{j} \cdot V(t)$, i.e. in the positive y-direction:

$$(x, y, t) \to \left(\xi = x, \eta = y - \int_0^t V(\widetilde{t})\, d\widetilde{t}, \tau = t\right), \tag{2.17a}$$

$$(u, v) \to (\widetilde{u} = u, \widetilde{v} = v - V(t)), \tag{2.17b}$$

where the tildes stand for the variables in new frame of reference (not to be mixed with the Laplace transform). Then the potential function ϕ transforms into $\widetilde{\phi} = \phi - V(t)\,\eta$, where we put the arbitrary time-dependent constant of integration to zero without loss of generality. Also, the partial derivatives are transformed according to

$$\partial_x = \partial_\xi, \;\; \partial_y = \partial_\eta, \;\; \partial_t = \partial_\tau - V\partial_\eta. \tag{2.18}$$

Since $V(t)$ is not constant, in general, this new coordinate system is non-inertial, and the nonlinear system (2.5) becomes

$$\text{bulk (velocity) } \eta \leqslant \widetilde{f}(\tau,\xi): \quad \begin{cases} \Delta\widetilde{\phi} = 0, \\ \nabla\widetilde{\phi} \to 0, \;\; \eta \to -\infty, \end{cases} \tag{2.19a}$$

$$\text{bulk (pressure) } \eta \leqslant \widetilde{f}(\tau,\xi): \quad \frac{\partial\widetilde{\phi}}{\partial\tau} + \frac{|\nabla\widetilde{\phi}|^2}{2} = -\frac{1}{\rho}p - \left(g + \frac{\mathrm{d}V}{\mathrm{d}\tau}\right)\eta + C(\tau), \tag{2.19b}$$

$$\text{interface (dynamic) } \eta = \widetilde{f}(\tau,\xi): \quad p = -\frac{\sigma\,\widetilde{f}_{\xi\xi}}{\left(1+\widetilde{f}_\xi^2\right)^{3/2}}, \tag{2.19c}$$

$$\text{interface (kinematic) } \eta = \widetilde{f}(\tau,\xi): \quad \frac{\partial\widetilde{f}}{\partial\tau} + \frac{\partial\widetilde{\phi}}{\partial\xi}\frac{\partial\widetilde{f}}{\partial\xi} = \frac{\partial\widetilde{\phi}}{\partial\eta}, \tag{2.19d}$$

where $\nabla = \boldsymbol{i}\,\partial_\xi + \boldsymbol{j}\,\partial_\eta$; $\widetilde{f} = f(t,x) - \int_0^t V(\widetilde{t})\,\mathrm{d}\widetilde{t}$ is the position of the interface in new coordinates; and purely time-dependent terms, namely $V^2/2$, are absorbed into the constant $C(\tau)$, (Equivalently, those terms can be absorbed in the pressure.) Since the base state corresponds to $p^0 \equiv 0$ at $\eta = 0$ and to $\widetilde{\phi}^0 \equiv 0$ and $\widetilde{f}^0 \equiv 0$, then $C(\tau) = 0$, and the pressure in the bulk is $p^0 = -\rho\,(g + \mathrm{d}V/\mathrm{d}t)\,\eta$. Imposing perturbations on this base state, $p = p^0 + p'$, $\widetilde{\phi} = \widetilde{\phi}^0 + \widetilde{\phi}'$, $\widetilde{f} = \widetilde{f}^0 + \widetilde{f}'$ and linearizing the corresponding equations (2.19), we arrive at the analogue of (2.9), but now in the non-inertial frame

$$\frac{\partial\widetilde{\phi}'}{\partial\tau} = -\frac{1}{\rho}p', \;\; \eta \leqslant 0, \tag{2.20a}$$

$$-\rho\left(g + \frac{\mathrm{d}V}{\mathrm{d}\tau}\right)\widetilde{f}' + p'|_{\eta=0} = -\sigma\,\widetilde{f}'_{\xi\xi}, \;\; \eta = 0, \tag{2.20b}$$

$$\frac{\partial\widetilde{f}'}{\partial\tau} = \frac{\partial\widetilde{\phi}'}{\partial\eta}, \;\; \eta = 0. \tag{2.20c}$$

As usual, the velocity potential is determined from the free-boundary problem for the Laplace equation:

$$\Delta\widetilde{\phi}' = 0, \;\; \eta \leqslant 0, \tag{2.21a}$$

$$\nabla\widetilde{\phi}' \to 0, \;\; \eta \to -\infty. \tag{2.21b}$$

Clearly, (2.21) produces $\overline{\phi} = A(s;k)\mathrm{e}^{|k|\eta}$ in the Fourier–Laplace space, where we adopted the notational conventions of §2.4. It is notable that system (2.20) differs from system (2.9) in the laboratory frame by the absence of a convective term, $V\widetilde{\phi}'_y$, in the Lagrange–Cauchy integral (2.20*a*). This difference leads to substantially different

stability results as can be seen from the resulting amplitude

$$A(s;k)=\frac{s(\widehat{\phi}(0;k;0)-V_0\widehat{f}(0;k))-\left[\sigma\frac{k^2}{\rho}+g\right]\widehat{f}(0;k)}{s^2+|k|\left[\sigma\frac{k^2}{\rho}+g\right]}, \tag{2.22}$$

which is obtained in the manner similar to that in § 2.4. While the reader can easily perform a general stability analysis analogous to the one in § 2.4, let us consider in detail the pure RM case, i.e. when constant acceleration and surface tension effects are absent. This leads to the following velocity potential amplitude and interfacial perturbation in the Fourier–Laplace space:

$$A(s;k)=\frac{-V_0\widehat{f}(0;k)+\widehat{\phi}(0;k;0)}{s},\quad \overline{f}(s;k)=|k|\frac{\widehat{\phi}(0;k;0)-V_0\widehat{f}(0;k)}{s^2}+\frac{\widehat{f}(0;k)}{s}. \tag{2.23}$$

As one can immediately infer from the first of these equations, the velocity potential is stable for any V_0. However, since $\mathscr{L}^{-1}[s^{-2}]=t$, the interface is linearly unstable with linear algebraic growth in agreement with the analysis of Richtmyer (1960). But, contrary to the conclusion of Richtmyer (1960), the growth rate is determined not only by $V_0\widehat{f}(0;k)$ (cf. (1.2)) but also by the initial perturbation of the velocity potential $\widehat{\phi}(0;k;0)$. The final question left is what are the reasons for the paradoxical difference in the stability results between moving frame of reference discussed in this section and the laboratory frame of reference analysed in § 2.4.

2.6. *Resolution of the paradox*

The resolution of the above paradox was actually given in the introduction: an observer moving with an interface does not discern whether the interface is accelerated or decelerated, while in the laboratory frame of reference the difference is obvious, which leads to the anisotropy. Below, we develop further intuition about this curious fact.

Let us use the index 'i' for the variables in the laboratory (inertial) frame of reference and 'n' for the variables in the moving (non-inertial) frame of reference. Clearly, the only difference between systems (2.9) and (2.20) – the presence of the extra convective term in (2.9a) – is the result of the transformation (2.17a). It is notable that the kinematic conditions (2.5d) and (2.20c) are not affected by this transformation in view of the absence of y-dependence. It is the goal of this subsection to reveal, with the help of simple examples, how this convective term may affect the growth rate measured in different frames of reference.

First, one can observe from the dependent variable transformation (2.17b) that perturbations in both coordinate frames of reference are equal at a given point in space–time,

$$f_i'=\widetilde{f}_n',\quad \phi_i'=\widetilde{\phi}_n',$$

as it should be: but this only adds more intrigue to the question as to why the time evolution of perturbations in these two frames are different. In order to appreciate this fact, let us consider a model problem in the laboratory frame,

$$\frac{\partial\varphi}{\partial t}+V\frac{\partial\varphi}{\partial y}=\lambda\varphi,\ \ V=\text{const}, \tag{2.24}$$

and look for a solution in the form $\varphi(t,y)=A(t)\mathrm{e}^{|k|y}$, recalling the special structure of the velocity potential solutions in our case (2.11). Then the time evolution is dictated

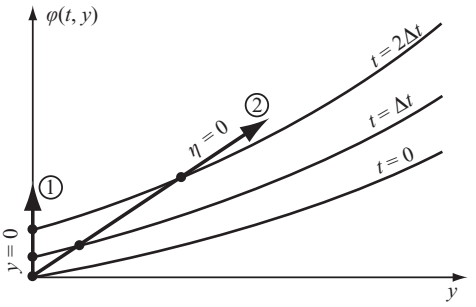

FIGURE 4. On a physical interpretation of the difference between growth rates in the laboratory, at $y=0$, and moving, at $\eta=0$, frames of reference for the solution of the model (2.24), $\varphi(t, y)=\mathrm{e}^{(\lambda-|k|V)t}\mathrm{e}^{y}$. Three solution curves correspond to three different times, $t=0,\ \Delta t,\ 2\Delta t$.

by the evolution of the amplitude A,

$$\frac{\mathrm{d}A}{\mathrm{d}t}=(\lambda-|k|V)A, \tag{2.25}$$

so that $\varphi\sim e^{(\lambda-|k|V)t}\mathrm{e}^{y}$. If, however, we transform to the frame of reference moving with speed V in y-direction,

$$(t, y)\rightarrow(\tau=t,\ \eta=y-V\,t);$$

then equation (2.24) becomes

$$\frac{\partial\varphi}{\partial\tau}=\lambda\varphi, \tag{2.26}$$

and therefore the growth rate in the (τ, η)-frame of reference is different, i.e. λ versus $\lambda-|k|V$. The solution for the amplitude $B(\tau)$ of $\phi(\tau, \eta)=B(\tau)\mathrm{e}^{|k|\eta}$ is $B(\tau)\sim\mathrm{e}^{\lambda\tau}$, i.e. $\varphi(\tau, \eta)\sim\mathrm{e}^{\lambda\tau}\mathrm{e}^{|k|\eta}$. However, it is obvious that the solutions are the same, but because of the special y-structure of the solution, i.e. the structure in the direction of translation of the frame of reference, the growth is seen differently in different frames of reference. This fact can be most easily appreciated with the help of a graphical interpretation in figure 4: if one measures the growth rate in the laboratory (t, y) frame of reference, e.g. at the location $y=0$ (arrow 1), then the growth rate is $\lambda-|k|V$, while if one moves with speed V in y-direction, then one measures the growth rate λ along the arrow 2. Again, this phenomenon is due to the exponential spatial y-structure of the solution, which makes it possible to add to or subtract from the exponential growth rate in time. One can imagine a situation in which the growth rate in time equals to and thus cancels the spatial growth rate of the solution in y-direction, as is the case for the RM instability and as illustrated by the example below. In this case the growth rate is not exponential anymore, i.e. $\mathrm{d}\varphi/\mathrm{d}t\sim\varphi(0)$, but may be algebraic due to linear amplification of non-zero initial conditions, $\varphi\sim\varphi(0)\cdot t$. The graphical interpretation in figure 4 also makes the origin of the asymmetry of the RM instability in the laboratory frame (i.e. the dependence of the growth rate on the sign of the shock velocity V_0, cf. §2.5) apparent: the observed growth rate depends on the sign of the velocity of the frame of reference. Namely, if the growth rate is isotropic in a particular frame, then it becomes anisotropic in the moving frame of reference. The above discussion reveals the effect of the Galilean part of the transformation (2.17*a*), while the contribution of the non-Galilean part – an impulsive acceleration – remains to be understood. One obvious effect of the non-inertial contribution is the origin of the isotropy of the RM instability in the frame of reference moving with the interface, as explained at the very beginning of this subsection: it follows from the symmetry

of the Dirac delta function, $\delta_D(-t)=\delta_D(t)$, since an observer sitting at a suddenly accelerated interface cannot discriminate between acceleration and deceleration.

In order to illustrate the fact that the growth can be algebraic in one reference frame and exponential in the other let us generalize example (2.24) to

$$\frac{\partial\varphi}{\partial t}+V\frac{\partial\varphi}{\partial y}=|k|V\varphi+f,\quad V=\text{const},$$
$$\frac{\partial f}{\partial t}=0.$$

If the solution, similar to our problem, has the structure $\varphi=A(t)\mathrm{e}^{|k|y}$, $f=B(t)\mathrm{e}^{|k|y}$, then the reader can easily find that the solution for $A(t)$ will be growing algebraically in the original reference frame while exponentially in the reference frame moving with velocity V.

What implications do the above examples have for the observation of the RM instability? For example, the drop splash problem develops the fingering instability – the famous crown – which is observed in the laboratory frame of reference (cf. figure 2). One can name a multitude of other physical phenomena, where the RM instability is important from the point of view of the laboratory observer but not the one who 'sits' on the interface. In this regard, the RT instability is also affected by this phenomenon of the different view of instability in the laboratory and coordinate frame moving with constant velocity, as one can observe from (2.13) and (2.22); however, if the reference frame is moving with the interface, i.e. accelerating, then the stability analyses are identical in both frames of reference for the RT case: the classical result of Taylor remains intact.

Finally, let us make an observation that in the laboratory frame both the velocity potential and the interface perturbation grow, as discussed in § 2.4, while in the moving frame of reference one of these may grow and the other may not, as we observed in § 2.5. To appreciate this basic fact in simple terms, let us consider system (2.9), i.e. in the laboratory frame, with vanishing g and σ and in the wavenumber space but with $V(t)$ of general time dependence, and look for the velocity potential solutions in the form $\widehat{\phi}(t, y)=A(t)\mathrm{e}^{|k|(y-f^0)}$. This results in a simple model problem

$$\frac{\mathrm{d}\widehat{f}}{\mathrm{d}t}=|k|A(t),$$
$$\frac{\mathrm{d}A}{\mathrm{d}t}+|k|VA=-\frac{\mathrm{d}V}{\mathrm{d}t}\widehat{f}.$$

Clearly, one of the first integrals of the above system, $A+V\widehat{f}=\text{const}$, demonstrates that if either A or $\widehat{f}$ grows or decays, then so does the other if $V=\text{const}\neq 0$. This is not the case in the moving frame of reference, as the analogous simplified analysis of (2.20) shows.

The result of this section on the stability of flat interfaces can be summarized as follows.

Assertion 1. *While the growth rate in the RT instability does not depend upon whether the phenomena are considered in the laboratory or accelerating with the interface frames of reference, the growth rate of the RM instability is algebraic in the frame moving with the interface and exponential in the laboratory frame of reference. The anisotropy of the RM instability with respect to the direction of the impulsive acceleration reveals itself only in the laboratory frame as opposed to the moving frame. In the pure RM case (no constant acceleration and surface tension effects), the system*

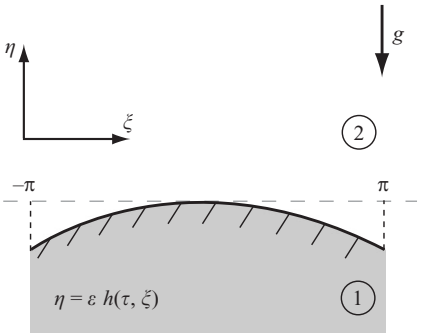

FIGURE 5. Curved interface as an $O(\epsilon)$ perturbation.

is exponentially unstable when the impulsive acceleration is directed towards lighter fluid and requires nonlinear stability analysis in the reversed situation.

Finally, it is worth mentioning that this effect has been masked by the natural limitations of current experimental accuracy and the $O(t^2)$ difference between linear $y(t) = y(0)(1 + \lambda t)$ and exponential $y(t) = y(0)\,\mathrm{e}^{\lambda t}$ growths. In fact, there are just a few experimental measurements for small times, i.e. when one can expect the linear mechanisms to govern the dynamics. For example, the data of Jones & Jacobs (1997) for low Mach numbers (figure 5 in their work) can be attributed to the linear (versus nonlinear) regime of the perturbation evolution at the most up to the times $t \sim 2\,\mathrm{ms}$ and thus do not allow one to distinguish linear algebraic from exponential growth due to the experimental scatter.

3. Two-dimensional curved interfaces

Since true base-state interfaces are frequently not flat and sometimes highly curved, such as the liquid rims discussed in the introduction, it is natural to explore possible deviations of the stability characteristics from those in the flat-interface case. Given the above understanding of the difference between observations in the laboratory and moving coordinate frames, from now on we choose to work in the frame of reference moving with an interface. Thus the starting point of the stability analysis of curved interfaces is system (2.19), and the key idea in this section is to consider the curved interface *locally*, as depicted in figure 5, with small deviation from flatness, i.e. $\widetilde{f}(\tau, \xi) = \epsilon h(\tau, \xi)$ with $\epsilon \ll 1$.

In what follows, for convenience, we will work with non-dimensional variables, which are introduced without new notations via $(\xi, \eta, \widetilde{f}) \to L(\xi, \eta, \widetilde{f})$, $\tau \to (L/a)^{1/2}\tau$, $\widetilde{\phi} \to L^{3/2}a^{1/2}\widetilde{\phi}$, $V \to (L\,a)^{1/2}V$, $p \to \rho L\,a\,p$, $g \to ag$, where L is the characteristic length scale of the physical system, e.g. capillary length $\sqrt{\sigma/\rho a}$ for liquid rims, and $a > 0$ is a suitable constant acceleration, e.g. in the pure RT case $a = |\mathrm{d}V/\mathrm{d}\tau|$. As a result of this non-dimensionalization, the effect of surface tension is expressed in terms of the Bond number $Bo = \rho L^2 a/\sigma$.

3.1. *Base state*

As one can infer from system (2.19), there exists a base-state solution of the following system:

$$\frac{\partial\widetilde{\phi}}{\partial\tau} + \frac{|\nabla\widetilde{\phi}|^2}{2} = Bo^{-1}\frac{\widetilde{f}_{\xi\xi}}{\left(1+\widetilde{f}_{\xi}^2\right)^{3/2}} - \left(g + \frac{\mathrm{d}V}{\mathrm{d}\tau}\right)\widetilde{f} + C(\tau), \tag{3.1a}$$

$$\frac{\partial\widetilde{f}}{\partial\tau} + \frac{\partial\widetilde{\phi}}{\partial\xi}\frac{\partial\widetilde{f}}{\partial\xi} = \frac{\partial\widetilde{\phi}}{\partial\eta}, \tag{3.1b}$$

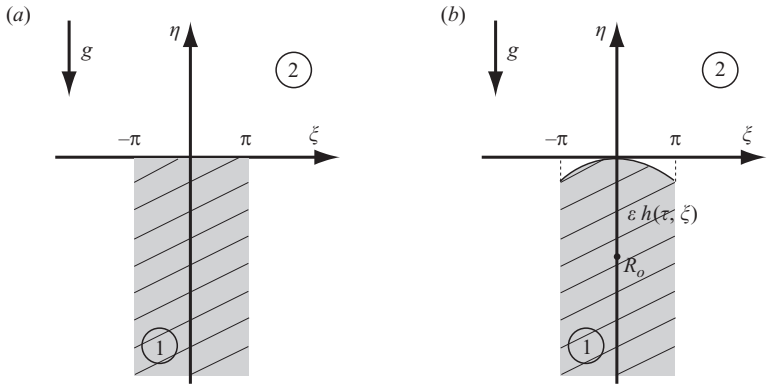

FIGURE 6. On constructing the potential function by the boundary perturbation method. (*a*) Semi-infinite flat column. (*b*) Semi-infinite column with curved tip.

which is motionless, $\widetilde{\phi}^0 = 0$, and steady, $\widetilde{f}^0(\xi)$, if the conditions of static equilibrium are met, i.e.

$$Bo^{-1}\frac{\widetilde{f}_{\xi\xi}}{\left(1+\widetilde{f}_{\xi}^2\right)^{3/2}} - \left(g + \frac{\mathrm{d}V}{\mathrm{d}\tau}\right)\widetilde{f} + C = 0, \tag{3.2}$$

where constant C is independent of time. Obviously, in this formulation, surface tension is required for the interface to have a non-zero curvature. In the RT case, $\mathrm{d}V/\mathrm{d}\tau = \mathrm{const}$ allows the corresponding balance of the capillary and hydrostatic pressures. In the RM case, i.e. when $V(\tau) = V_0\, H(\tau)$, we have $\widetilde{f}(\tau, \xi) \equiv \widetilde{f}^0(\xi)$ and $\phi(\tau, \xi, \eta) \equiv 0$ for $\tau \leqslant 0$. For $\tau > 0$, these are also the solutions, since we have already transformed to the frame of reference moving with velocity $V(\tau)$. In other words, we consider the interface and the bulk within it (at least in the very neighbourhood of the interface with the highest curvature) as moving translationally with $V(\tau)$ as a single whole.

The final question is the existence of an interface with a non-zero curvature. While (3.2) can be reduced to quadratures, the existence of such surface with non-zero second derivative $\widetilde{f}_{\xi\xi}$ can be demonstrated by substituting an even power series representation,

$$\widetilde{f}^0(\xi) = \epsilon h^0(\xi) = \epsilon \sum_{i=1}^{\infty} c_{2i}\xi^{2i}, \tag{3.3}$$

and showing that there is a non-trivial solution for the coefficients, c_{2i}.

3.2. *Construction of the potential function*

As it was pointed out in § 2.4, it is important to be able to construct a general solution of the Laplace equation with non-fixed boundary values:

$$\begin{gathered}\Delta\phi = 0,\\ \eta = \epsilon h(\xi):\ \phi = \Phi(\xi),\end{gathered} \tag{3.4}$$

where $\Phi(\xi)$ is an arbitrary summable function to be determined from the free-boundary conditions. Without loss of generality, let the width of the domain be 2π (in non-dimensional coordinates, cf. figure 6). If one restricts the consideration to even functions $h(\xi)$, then, for example, reasonable approximations are $\epsilon h^0(\xi) \simeq -\xi^2/(2R_0)$, where $R_0 \gg \pi$ is the radius of curvature, or $h^0(\xi) = \cos\xi - 1$. The *key idea* is to consider the region in the neighbourhood of the interface with the largest curvature, as sketched in figure 5, and construct the most general velocity potential, which

satisfies the Laplace equation in this region and allows one to solve the free-boundary problem. This constitutes the essence of the *local approach*. Since we are interested in a small, $O(\epsilon)$, perturbation of the boundary (cf. figure 5), it is natural to appeal to the boundary perturbation method (although another more cumbersome approach would be to use the conformal mapping technique). The basic idea of this method (Dyke 1975) is to transform the boundary conditions on the *perturbed* boundaries to that on the *unperturbed* boundaries, which are known.

Therefore, consider a sequence of two problems, a semi-infinite flat column and a semi-infinite column with a curved tip, sketched in figures 6(a) and 6(b). First, we expand the potential function in powers of ϵ:

$$\phi(\xi, \eta) = \phi^{(0)} + \epsilon\, \phi^{(1)} + \dots, \tag{3.5}$$

where time dependence is suppressed for a moment, since at this stage we are constructing a solution to the Laplace equation. Second, we expand the solution at the boundary:

$$\phi(\xi, \eta)|_{\eta=\epsilon h(\xi)} = \phi(\xi, 0) + \epsilon h(\xi)\frac{\partial \phi}{\partial \eta}(\xi, 0) + \dots. \tag{3.6}$$

Then, approximating the solution of (3.4), we get two problems, for the zero- and first-order approximations:

zero order:

$$\begin{gathered} \Delta\phi^{(0)} = 0, \\ \eta = 0 : \ \phi^{(0)} = \Phi(\xi), \end{gathered} \tag{3.7}$$

first order:

$$\begin{gathered} \Delta\phi^{(1)} = 0, \\ \eta = 0 : \ \phi^{(1)} = h(\xi)\tfrac{\partial \phi^{(0)}}{\partial \eta}(\xi, 0). \end{gathered} \tag{3.8}$$

The zero-order approximation (3.7) yields

$$\phi^{(0)}(\xi, \eta) = \sum_{n=-\infty}^{+\infty} A_n^{(0)} \mathrm{e}^{|n|\eta} \mathrm{e}^{in\xi}, \tag{3.9}$$

where the amplitudes $A_n^{(0)}$ are found from the boundary condition at $\eta = 0$: $\phi^{(0)}(\xi, 0) = \Phi(\xi) = \sum_{n=-\infty}^{+\infty} A_n^{(0)} \mathrm{e}^{in\xi}$. Since $\Phi(\xi)$ is summable, $\partial\phi^{(0)}/\partial\xi$ is summable (convergent) as well. Then, the first-order approximation (3.8) produces the analogous solution

$$\phi^{(1)}(\xi, \eta) = \sum_{n=-\infty}^{+\infty} A_n^{(1)} \mathrm{e}^{|n|\eta} \mathrm{e}^{in\xi}, \tag{3.10}$$

where the amplitudes $A_n^{(1)}$ are found from the boundary condition at $\eta = 0$, that is by equating $\sum_{n=-\infty}^{+\infty} A_n^{(1)} \mathrm{e}^{in\xi} = h(\xi) \sum_{n=-\infty}^{+\infty} A_n^{(0)} |n| \mathrm{e}^{in\xi}$. For example, if $h(\xi) = \cos\xi - 1$, then

$$A_n^{(1)} = A_n^{(0)} + \frac{1}{2}\left\{(n-1)A_{n-1}^{(0)} + (n+1)A_{n+1}^{(0)}\right\}. \tag{3.11}$$

The main conclusion is that despite the fact that the boundary is curved, as in figure 6(b), finite Fourier modes $\mathrm{e}^{in\xi}$ constitute a complete set of functions and thus allow one to build the solution to (3.4), which from now on will be represented in the

general form,

$$\phi(\tau,\xi,\eta)=\sum_{n=-\infty}^{+\infty}A_n(\tau)\mathrm{e}^{|n|\eta}\mathrm{e}^{in\xi}, \tag{3.12}$$

where we restored time dependence previously suppressed. In this context, it is natural to comment on the *ad hoc* idea of Layzer (1955), which provided a breakthrough in the nonlinear modelling of the RT and RM instabilities. Layzer suggested approximating the potential function by $\phi(\tau,\xi,\eta)=A(\tau)\mathrm{e}^{\eta}\cos\xi$ near the tip of the bubble, which, apparently, is just one harmonic with $n=1$ out of the general expression (3.12) and which allowed him to derive a nonlinear evolution equation for the bubble amplitude $A(\tau)$. Using more terms from (3.12) one can get a more accurate nonlinear model.

3.3. *Linearized equations*

The equations for perturbations linearized around the curved non-perturbed interface $\widetilde{f}^0(\xi)$ in the frame moving with the interface are given by

$$\frac{\partial\widetilde{\phi}'}{\partial\tau}=-p',\ \ \eta\leqslant\widetilde{f}^0(\xi), \tag{3.13a}$$

$$-\left(g+\frac{\mathrm{d}V}{\mathrm{d}\tau}\right)\widetilde{f}'+p'=-Bo^{-1}\left[\frac{\widetilde{f}'_{\xi\xi}}{\left(1+\widetilde{f}^{0\,2}_{\xi}\right)^{3/2}}-3\frac{\widetilde{f}^0_{\xi}\widetilde{f}^0_{\xi\xi}}{\left(1+\widetilde{f}^{0\,2}_{\xi}\right)^{5/2}}\widetilde{f}'_{\xi}\right],\ \ \eta=\widetilde{f}^0(\xi), \tag{3.13b}$$

$$\frac{\partial\widetilde{f}'}{\partial\tau}+\frac{\partial\widetilde{f}^0}{\partial\xi}\frac{\partial\widetilde{\phi}'}{\partial\xi}=\frac{\partial\widetilde{\phi}'}{\partial\eta},\ \ \eta=\widetilde{f}^0(\xi). \tag{3.13c}$$

Since $\widetilde{f}^0(\xi)=\epsilon h^0(\xi)$, keeping the terms up to $O(\epsilon)$ and excluding pressure in (3.13), we arrive at the following system of two equations at $\eta=\epsilon h^0(\xi)$:

$$\frac{\partial\widetilde{\phi}'}{\partial\tau}=-\left(g+\frac{\mathrm{d}V}{\mathrm{d}\tau}\right)\widetilde{f}'+Bo^{-1}\widetilde{f}'_{\xi\xi}+o(\epsilon), \tag{3.14a}$$

$$\frac{\partial\widetilde{f}'}{\partial\tau}=-\epsilon\frac{\partial h^0}{\partial\xi}\frac{\partial\widetilde{\phi}'}{\partial\xi}+\frac{\partial\widetilde{\phi}'}{\partial\eta}. \tag{3.14b}$$

It is natural to expect that the term of $O(\epsilon)$ should introduce a non-trivial correction to the results of § 2.

3.4. *Stability analysis: the RT case*

For the sake of mathematical clarity, let us first consider the case of the RT instability, i.e. $\mathrm{d}V/\mathrm{d}\tau=-1$, since we are interested in the unstable configuration. In this case, system (3.14) contains no explicit time dependence, and therefore one can perform the standard eigenvalue analysis,

$$(\widetilde{\phi}'(\tau,\xi),\widetilde{f}'(\tau,\xi))\rightarrow(\Phi(\xi),F(\xi))\,\mathrm{e}^{\lambda\tau}, \tag{3.15}$$

which, after eliminating $F(\xi)$, produces

$$\lambda^2\Phi=-(g-1)\left[\Phi_\eta-h^0_\xi\Phi_\xi\right]+Bo^{-1}\left[\Phi_{\xi\xi\eta}-h^0_{\xi\xi\xi}\Phi_\xi-2h^0_{\xi\xi}\Phi_{\xi\xi}-h^0_\xi\Phi_{\xi\xi\xi}\right]. \tag{3.16}$$

Next, the analysis is based on the well-established operator perturbation theory (Kato 1966), which allows one to treat this problem as a regular (non-singular) perturbation problem,

$$\Phi(\xi)=\Phi^0+\epsilon\Phi^1+o(\epsilon),\ \ \lambda=\lambda_0+\epsilon\lambda_1+o(\epsilon), \tag{3.17}$$

which yields

$$\epsilon^0 : \lambda_0^2 \Phi^0 + (g-1)\Phi_\eta^0 - Bo^{-1}\Phi_{\xi\xi\eta}^0 = 0, \tag{3.18a}$$

$$\epsilon^1 : \lambda_0^2 \Phi^1 + (g-1)\Phi_\eta^1 - Bo^{-1}\Phi_{\xi\xi\eta}^1 = -2\lambda_0\lambda_1\Phi^0 + (g-1)h_\xi^0\Phi_\xi^0 - Bo^{-1}\left[h_{\xi\xi\xi}^0\Phi_\xi^0 + 2h_{\xi\xi}^0\Phi_{\xi\xi}^0 + h_\xi^0\Phi_{\xi\xi\xi}^0\right]. \tag{3.18b}$$

Based on the results of § 3.2, potentials are given by

$$\Phi^i(\xi,\eta) = \sum_{n=-\infty}^{+\infty} A_n^i \mathrm{e}^{|n|\eta}\mathrm{e}^{in\xi}. \tag{3.19}$$

Then, substituting the zero-order approximation $\Phi^0(\xi,\eta)$ in (3.18*a*), evaluating at $\eta = 0$ and projecting onto $\mathrm{e}^{im\xi}$ yields

$$\lambda_{\pm 0}^2 = -(g-1)|n| - Bo^{-1}|n|^3, \tag{3.20}$$

which is the dispersion relation governing the stability of a two-dimensional column with a flat top, as in figure 6(*a*). Next, substitution of $\Phi^1(\xi,\eta)$ into (3.18*b*) and projection† onto $\mathrm{e}^{im\xi}$ leads to vanishing of the left-hand side of (3.18*b*) in view of the definition of the zero-order eigenvalue (3.20), while the rest of (3.18*b*) results in

$$4\pi\lambda_0\lambda_1 A_m^1 = \sum_n A_n^1 \int_{-\pi}^{\pi} \left\{ \mathrm{i}n(g-1)h_\xi^0 - Bo^{-1}\left[\mathrm{i}nh_{\xi\xi\xi}^0 - 2n^2 h_{\xi\xi}^0 - \mathrm{i}n^3 h_\xi^0\right]\right\} \mathrm{e}^{i(n-m)\xi}\,\mathrm{d}\xi.$$

Since $\widetilde{\phi}'(\tau,\xi)$ is real, thus making $\Phi^i(\xi,\eta)$ real as well, $A_{-r} = A_r$ and thus expansions (3.19) contain only cosines. Since $h^0(\xi)$ and $h_{\xi\xi}^0(\xi)$ are even functions of ξ, with $h_\xi^0(\xi)$ and $h_{\xi\xi\xi}^0(\xi)$ being the odd functions, integrals involving $h_\xi^0(\xi)$ and $h_{\xi\xi\xi}^0(\xi)$ should vanish. The only terms left are

$$4\pi\lambda_0\lambda_1 A_m^1 = 2Bo^{-1}\sum_n A_n^1 \int_{-\pi}^{\pi} n^2 h_{\xi\xi}^0 \mathrm{e}^{i(n-m)\xi}\,\mathrm{d}\xi. \tag{3.21}$$

Since we perform the *local analysis*, $h_{\xi\xi}^0 \simeq \kappa = \text{const}$ is the scaled $O(1)$ curvature, and based on (3.21), the first approximation for the eigenvalue becomes

$$\lambda_{\pm 1}^{(n)} \simeq Bo^{-1}\frac{n^2}{\lambda_{\pm 0}^{(n)}}\int_{-\pi}^{\pi} h_{\xi\xi}^0\,\mathrm{d}\xi, \tag{3.22}$$

where we used the orthogonality of the Fourier modes, $\mathrm{e}^{in\xi}$. Note that if the interface is non-symmetric, i.e. the odd derivatives $h_\xi^0(\xi)$ and $h_{\xi\xi\xi}^0(\xi)$ do not vanish, then these will affect the eigenvalue corrections; here we consider the symmetric case as the leading-order effect. Hence, we have proved the following Assertion.

Assertion 2. *If the flat interface is unstable in the RT case, i.e. there exists real* $\lambda_{+0}^{(n)} > 0$, *then the addition of a positive curvature (concave interface; cf. figure 7a) makes the physical system more unstable, while the addition of negative curvature (convex interface; cf. figure 7b) makes the system less unstable. The eigenvalues obey*

$$\lambda_{\pm}^{(n)} = \lambda_{\pm 0}^{(n)} + \epsilon\lambda_{\pm 1}^{(n)} + o(\epsilon), \tag{3.23}$$

where $\lambda_{\pm 0}^{(n)}$ *and* $\lambda_{\pm 1}^{(n)}$ *are given by (3.20) and (3.22), respectively.*

† Alternatively, the problem of finding the eigenvalue perturbation can be done with the help of the adjoint eigenvalue problem.

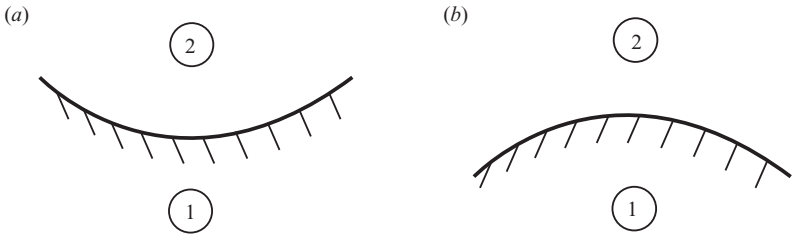

FIGURE 7. Two generic curved interfaces; phase 1 is the (heaviest) liquid phase. (*a*) Concave interface: $\kappa > 0$. (*b*) Convex interface: $\kappa < 0$.

In order to appreciate these results, let us make the following few corollary-type clarifications: First, the flat-interface results, given by the growth rates (3.20), are trivially recovered in the limit of vanishing base-state curvature $\kappa \to 0$, i.e. $\epsilon \to 0$; the same applies to the subsequent results for the RM instability and three-dimensional interfaces. Note that while the base-state curvature considered in this paper is due to the presence of surface tension (for the sake of concreteness), this study should have analogous implications for the stability characteristics regardless of the physical origins of the base-state curvature, which signifies the geometrical nature of the found effects. Second, the interpretation of these curvature effects is not as trivial as one might think (i.e. that the presence of surface tension tends to flatten the interface, since the curved-interface base state is truly an equilibrium base state). Third, because of the curvature effect, the RT instability can be reversed; i.e. the sign of the growth rate can change as a function of base-state curvature. Indeed, if the heavy phase 1 accelerates the light phase 2 and if the interface is flat, then there should be no instability according to the RT criterion; however, if the interface is concave (cf. figure 7*a*), then the instability may appear. In fact, the above two points can be illustrated with the well-known phenomena of vapour-filled underwater collapsing bubbles (Birkhoff 1954; Plesset 1954), which are unstable despite that the denser liquid is accelerating the lighter vapour. This problem of underwater collapsing bubbles has been studied exactly because of its spherical symmetry. Similar effects were found in the problems of radially imploding/exploding spherical (Mikaelian 1990) and cylindrical (Mikaelian 2005) shells. However, to the author's knowledge the fact that this is a particular case of the more general effect of interfacial curvature has never been established.

Lastly, it is known that the RT theory is valid only in the small amplitude limit, but when the interfacial distortions become significant the rate of their growth deviates substantially from the one predicted by the RT theory (Lewis 1950). Apparently, one of the sources of these deviations is finger formation and thus non-zero curvature: the fingers can be considered, in a quasi-static approximation, as a new base state which is subject to perturbations. The latter will have growth rate different from the case of a flat-interface base state, as we just demonstrated.

3.5. *Stability analysis: the RM case*

The stability characteristics of curved interfaces in the RM case are more complicated than in the RT case. Here we consider the 'pure' RM case, which in the situation of curved interfaces requires the presence of surface tension; otherwise, non-trivial $h^0(\xi)$ would not exist. In view of the time dependence of $V(\tau)$, the stability analysis will naturally be performed in the Laplace transform space with the idea to determine the perturbed location of singularities in the complex plane of s.

First, consider the problem in the frame of reference moving with the interface. Then the starting point is system (3.14) with $g=0$ and $V(\tau)=V_0H(\tau)$. Let the Laplace transform of $\widetilde{\phi}'$ be denoted by $\Phi(s;\xi,\eta)$ and that of $\widetilde{f}'$ by $F(s;\xi,\eta)$. Then, applying the Laplace transform to (3.14) and eliminating $F(s;\xi,\eta)$, we find

$$s^2\Phi(s)-s\widetilde{\phi}'(0)=-sV_0\widetilde{f}'(0) + Bo^{-1}\left[\widetilde{f}'_{\xi\xi}(0)+\Phi_{\xi\xi\eta}-\epsilon\left(h^0_{\xi\xi\xi}\Phi_\xi+2h^0_{\xi\xi}\Phi_{\xi\xi}+h^0_\xi\Phi_{\xi\xi\xi}\right)\right]. \quad (3.24)$$

Since the problem for the potential function has the solution

$$\Phi(s;\xi,\eta)=\sum_n A_n e^{|n|\eta}e^{in\xi} \quad (3.25)$$

in the curved region, one finds that the location of singularities is dictated by the quadratic equation

$$s^2=Bo^{-1}n^2(2\epsilon\kappa-|n|), \quad \text{where } \kappa=\int_{-\pi}^{\pi}h^0_{\xi\xi}\,d\xi. \quad (3.26)$$

Clearly, within the asymptotic approximation, $\epsilon\ll 1$, the perturbation potential function should be neutrally stable in the moving frame of reference. However, one might guess that it may become unstable for high enough curvature κ.

Now, let us look at the problem in the laboratory frame of reference. Performing calculations analogous to the above analysis, one ends up with the following formula for the location of singularities:

$$s^2+|n|[Bo^{-1}n^2+sV_0]-2\epsilon n^2\kappa Bo^{-1}=0. \quad (3.27)$$

For clarity, let us expand $s=s_0+\epsilon s_1+o(\epsilon)$; then one finds

$$s_0=\pm\sqrt{-|n|[Bo^{-1}n^2+sV_0]}, \quad s_1=\frac{2n^2\kappa Bo^{-1}}{2s_0+|n|V_0}. \quad (3.28)$$

The latter expression indicates that even if in the absence of curvature ($\kappa\equiv 0$) the perturbation velocity field is not growing in time, i.e. s_0 is imaginary, the addition of a non-zero curvature leads to either stabilization or destabilization depending upon the sign of κ. Also, the addition of interfacial curvature may either enhance or suppress an already-unstable perturbation velocity field. The results of this subsection can be summarized as follows.

ASSERTION 3. *The neutrally stable flat interface under the condition of impulsive acceleration may become either exponentially stable or unstable in the laboratory frame of reference, depending upon the sign of the added interfacial curvature.*

4. Three-dimensional curved interfaces

With the above understanding of the stability of two-dimensional flat and weakly curved interfaces, one can address the stability of three-dimensional rims, as motivated by figure 2. Naturally, the main question of interest is the rim instability along ξ-axis, as shown schematically in figure 8. The idea of the stability analysis is the same as in § 3, i.e. to analyze the structure of the solution near the rim tip, so that *locally* it is almost flat with $O(\epsilon)$ curvature. Then, the translation of the results of the previous

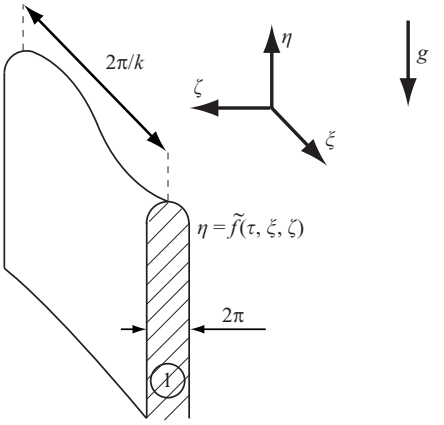

FIGURE 8. Three-dimensional rim.

section onto the three-dimensional case turns out to be straightforward, as suggested by the structure of the velocity potential solution, i.e. the solution of the problem analogous to (3.4):

$$\begin{gathered}\Delta\phi = 0,\\ y = \epsilon h(\xi) : \ \phi = \Phi(\xi, \zeta).\end{gathered} \tag{4.1}$$

The zero- and first-order approximations read

$$\phi^{(j)}(\tau, \xi, \eta, \zeta) = \int_{\mathbb{R}} \sum_{n=-\infty}^{+\infty} A_n^{(j)}(\tau) \mathrm{e}^{ik\xi} \mathrm{e}^{\sqrt{k^2+|n|^2}\eta} \mathrm{e}^{in\zeta} \, \mathrm{d}k, \ \ j = 1, \ 2, \tag{4.2}$$

and therefore, as can be easily determined, one gets the eigenvalue approximations $\lambda_{\pm 0}^{(n)}$ and $\lambda_{\pm 1}^{(n)}$ analogous to (3.20) and (3.22):

$$\lambda_{\pm 0}^{(n)} = \pm\big[-(g-1)\sqrt{k^2+|n|^2} - Bo^{-1}(k^2+|n|^2)^{3/2}\big]^{1/2}, \tag{4.3a}$$

$$\lambda_{\pm 1}^{(n)} \simeq Bo^{-1} \frac{n^2}{\lambda_{\pm 0}^{(n)}} \int_{-\pi}^{\pi} h_{\zeta\zeta}^0 \, \mathrm{d}\zeta\,; \tag{4.3b}$$

i.e. the only difference is that the discrete wavenumber, n, (in ζ-direction) in (3.20) is replaced with the wavenumber in the (ξ, ζ)-plane, $\sqrt{k^2+|n|^2}$. This fact and (4.2) for the perturbation velocity field allow one to clearly see the energy argument made in § 1.2: the curvature affects the depth of penetration of a disturbance into the bulk, and thus the factor $|k|$ in (1.1) and (1.2) is modified. In fact, for the long-wave perturbations of a rim of a liquid sheet of thickness 2π, i.e. when $|k|^{-1} \gg 2\pi$, the depth of penetration is $\sim 2\pi$ and therefore the factor $|k|$ in (1.1) and (1.2) is replaced by $(2\pi)^{-1}$. The latter of course affects the growth rate and the wavenumber selection. Since, the eigenvalue has the structure

$$\lambda = \lambda_0(k; n) + C(n)\kappa, \tag{4.4}$$

where κ is the curvature, the curvature in ζ-direction has an effect on the wavenumber selection in ξ-direction (cf. figure 9). For example, convex interfaces stabilize the physical system and narrow the range of unstable wavenumbers. Also, the effect of increasing surface tension (or, equivalently, decreasing Bo) is not only to stabilize

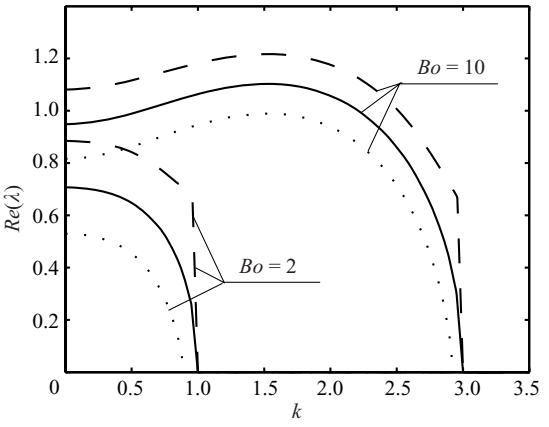

FIGURE 9. Effect of the interfacial curvature on the eigenvalues in the three-dimensional case for $g = 0$, $\epsilon = 0.02$, $\kappa = \pm 1.0$, $n = 1$ and two values of Bond number, $Bo = 2$ and $Bo = 10$ in (4.4). Solid curve corresponds to zero curvature, dashed line to concave interface and dotted line to convex interface.

short wavelengths, as known (see solid lines in figure 9) from the classical theory of Drazin & Reid (2004), but also to amplify the stabilizing or destabilizing effect of curvature depending upon its sign, as suggested by figure 9. Thus, the analysis of three-dimensional curved interfaces can be summarized as follows.

ASSERTION 4. *The stability of three-dimensional rims, as that shown in figure 8, is affected by the transverse curvature: concave interfaces are less stable than flat ones, while convex interfaces are more stable. The range of lengthwise-unstable wavenumbers (i.e. along-the-rim wavenumbers) is narrowed in the case of convex interfaces.*

5. Conclusions

In this work, increased understanding of the RM instability was gained, which uncovered important particulars missing in Richtmyer's original treatment, including the effects of reference frames and initial velocity field perturbations. The second main contribution of this study is the clarification of the interfacial curvature effects in the two-dimensional and three-dimensional cases on the development of the RT and RM instabilities, as well as on the unstable wavenumbers selection. All the major results are summarized in Assertions 1–4. The analysis of the stability of curved interfaces also led to the rigorous generalization of the classical idea of Layzer (1955) on approximating the potential function in free-boundary problems with curved base-state interfaces. The key ingredients of the approach are the linear operator and the boundary perturbation theories.

Since in three dimensions a curved interface is characterized by two principal curvatures (Spivak 1999), the three-dimensional case leaves some open questions, in particular the effects of the second curvature R_2^{-1}, as illustrated in figure 10: namely the stability characteristics of a rim bent in the transverse (cf. figure 10*a*) and the longitudinal (cf. figure 10*b*) directions are not understood yet. Finally, it would also be interesting to analyze the general case of time-dependent accelerations, i.e. in between the constant and impulsive ones.

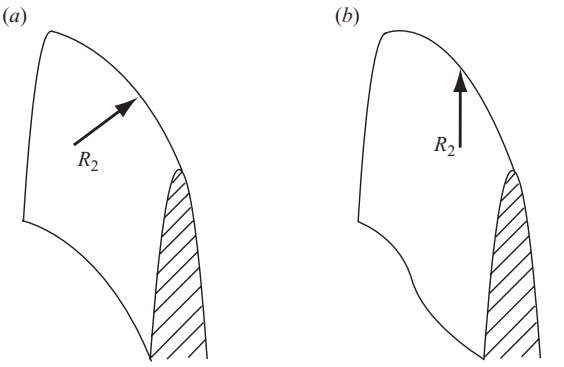

FIGURE 10. On the presence of second curvature in the three-dimensional case.

This work was supported by NSERC Discovery Grant 341849-2007. The author gratefully acknowledges the hospitality he enjoyed during his stay at the University of Alberta, where this work was completed, along with useful feedback and encouraging discussions with Professor Bud Homsy and valuable comments of the referees.

REFERENCES

ARNETT, D. 2000 The role of mixing in astrophysics. *Astrophys. J.* **127** (Suppl.), 213–217.

ARONS, J. & LEA, S. M. 1976 Accretion onto magnetized neutron stars: structure and interchange instability of a model magnetosphere. *Astrophys. J.* **207**, 914–936.

BATCHELOR, G. K. 1967 *An Introduction to Fluid Dynamics*. Cambridge University Press.

BIRKHOFF, G. 1954 Note on Taylor instability. *Quart. Appl. Math.* **12**, 306–309.

BROUILLETTE, M. 2002 The Richtmyer–Meshkov instability. *Annu. Rev. Fluid Mech.* **34**, 445–468.

CARLÉS, P. & POPINET, S. 2002 The effect of viscosity, surface tension and non-linearity on Richtmyer–Meshkov instability. *Euro. J. Mech.* B **21**, 511–526.

CATTANEO, F. & HUGHES, D. W. 1988 The nonlinear breakup of a magnetic layer: instability to interchange modes. *J. Fluid Mech.* **196**, 323–344.

DRAZIN, P. G. & REID, W. H. 2004 *Hydrodynamic stability*. Cambridge University Press.

DYKE, M. VAN 1975 *Perturbation Methods in Fluid Mechanics*. Parabolic Press.

FRALEY, G. 1986 Rayleigh–Taylor stability for a normal shock wave-density discontinuity interaction. *Phys. Fluids* **29**, 376–386.

FRIEMAN, E. A. 1954 On elephant-trunk structures in the region of O-associations. *Astrophys. J.* **120**, 18–21.

GROVE, J. W., HOLMES, R., SHARP, D. H., YANG, Y. & ZHANG, Q. 1993 Quantitative theory of Richtmyer–Meshkov instability. *Phys. Rev. Lett.* **71**, 3473–3476.

HAZAK, G. 1996 Lagrangian formalism for the Rayleigh–Taylor instability. *Phys. Rev. Lett.* **76**, 4167–4170.

HECHT, J., ALON, U. & SHVARTS, D. 1994 Potential flow models of Rayleigh–Taylor and Richtmyer–Meshkov bubble fronts. *Phys. Fluids* **6**, 4019–4030.

JONES, M. A. & JACOBS, J. W. 1997 A membraneless experiment for the study of Richtmyer–Meshkov instability of a shock-accelerated gas interface. *Phys. Fluids* **9**, 3078–3085.

KATO, T. 1966 *Perturbation Theory for Linear Operators*. Springer.

KHOKHLOV, A. M., ORAN, E. S. & THOMAS, G. O. 1999 Numerical simulation of deflagration-to-detonation transition: the role of shock-flame interactions in turbulent flames. *Combust. Flames* **117**, 323–329.

KRECHETNIKOV, R. & HOMSY, G. M. 2009 Crown-forming instability phenomena in the drop splash problem. *J. Colloid Interface Sci.* **331**, 555–559.

LANDAU, L. D. & LIFSHITZ, E. M. 1987 *Fluid Mechanics*. Pergamon.

Lawrentjew, M. A. & Schabat, B. V. 1967 *Methoden der komplexen Funktionentheorie*. Deutscher Verlag der Wissenschaften.

Layzer, D. 1955 On the instability of superimposed fluids in a gravitational field. *Astrophys. J.* **122**, 1–12.

Lewis, D. J. 1950 The instability of liquid surfaces when accelerated in a direction perpendicular to their planes. Part 2. *Proc. R. Soc.* A **202**, 81–96.

Lindl, J. D. & Mead, W. C. 1975 2-dimensional simulation of fluid instability in laser-fusion pellets. *Phys. Rev. Lett.* **34**, 1273–1276.

Meshkov, E. E. 1969 Instability of the interface of two gases accelerated by a shock wave. *Sov. Fluid. Dyn.* **4**, 101–108.

Mikaelian, K. O. 1990 Rayleigh–Taylor and Richtmyer–Meshkov instabilities and mixing in stratified spherical shells. *Phys. Rev.* A **42**, 3400–3420.

Mikaelian, K. O. 1994 Freeze-out and the effect of compressibility in the Richtmyer–Meshkov instability. *Phys. Fluids* **6**, 356–368.

Mikaelian, K. O. 1998 Analytic approach to nonlinear Rayleigh–Taylor and Richtmyer–Meshkov instabilities. *Phys. Rev. Lett.* **80**, 508–511.

Mikaelian, K. O. 2005 Rayleigh–Taylor and Richtmyer–Meshkov instabilities and mixing in stratified cylindrical shells. *Phys. Fluids* **17**, 094105.

Ott, E. 1972 Nonlinear evolution of the Rayleigh–Taylor instability of a thin layer. *Phys. Rev. Lett.* **20**, 1429–1432.

Plesset, M. S. 1954 On the stability of fluid flows with spherical symmetry. *J. Appl. Phys.* **25**, 96–98.

Rayleigh, L. 1883 Investigation of the character of the equilibrium of an incompressible heavy fluid of variable density. *Proc. Lond. Math. Soc.* **14**, 170–177.

Richtmyer, R. D. 1960 Taylor instability in shock acceleration of compressible fluids. *Comm. Pure Appl. Math.* **XIII**, 297–319.

Sazonov, S. V. 1991 Dissipative structures in the f-region of the equatorial ionosphere generated by Rayleigh–Taylor instability. *Planet. Space Sci.* **39**, 1667–1671.

Sharp, D. H. 1984 An overview of Rayleigh–Taylor instability. *Physica* D **12**, 3–18.

Sirignano, W. A. & Mehring, C. 2000 Review of theory of distortion and disintegration of liquid streams. *Prog. Energy Combust. Sci.* **26**, 609–655.

Spivak, M. 1999 *A Comprehensive Introduction to Differential Geometry*. Publish or Perish Press.

Taylor, G. I. 1950 The instability of liquid surfaces when accelerated in a direction perpendicular to their planes. Part 1. Waves on fluid sheets. *Proc. R. Soc. Lond.* A **201**, 192–196.

Velikovich, A. L. & Dimonte, G. 1996 Nonlinear perturbation theory of the incompressible Richtmyer–Meshkov instability instability. *Phys. Rev. Lett.* **76**, 3112–3115.

Wilcock, W. S. D. & Whitehead, J. A. 1991 The Rayleigh–Taylor instability of an embedded layer of low-viscosity fluid. *J. Geophys. Res.* **96**, 12193–12200.

Wouchuk, J. G. & Nishihara, K. 1996 Linear perturbation growth at a shocked interface. *Phys. Plasmas* **3**, 3761–3776.

Yang, Y., Zhang, Q. & Sharp, D. H. 1994 Small amplitude theory of Richtmyer–Meshkov instability. *Phys. Fluids* **6**, 1856–1873.